Article

Not peer-reviewed version

Enhanced Electromagnetic Wave Absorption Properties of FeCo-C Alloy by Exploiting Metamaterial Structure

Tang Xuan Duong , Do Khanh Tung , Bui Xuan Khuyen , Nguyen Thi Ngoc Anh , Bui Son Tung , Vu Dinh Lam , Liangyao Chen , Haiyu Zheng , YoungPak Lee *

Posted Date: 6 June 2023

doi: 10.20944/preprints202306.0371.v1

Keywords: metamaterials; broad-band absorption; iron-cobalt alloy; electromagnetic coupling

Article

Enhanced Electromagnetic Wave Absorption Properties of FeCo-C Alloy by Exploiting Metamaterial Structure

Tang Xuan Duong [1,2,3], Do Khanh Tung [1, 2,], Bui Xuan Khuyen [1,2], Nguyen Thi Ngoc Anh [2], Bui Son Tung [1,2,**], Vu Dinh Lam [1], Liangyao Chen [4], Haiyu Zheng [5,6] and YoungPak Lee [4,5,6,*]**

[1] Graduate University of Science and Technology, Vietnam Academy of Science and Technology, 18 Hoang Quoc Viet, Hanoi 100000, Vietnam, lamvd@gust-edu.vast.ac.vn (V.D.L.)
[2] Institute of Materials Science, Vietnam Academy of Science and Technology, 18 Hoang Quoc Viet, Hanoi 100000, Vietnam, khuyenbx@ims.vast.ac.vn (B.X.K.); anhntn@ims.vast.ac.vn (N.T.N.A)
[3] Joint Russia-Vietnam Tropical Science and Technology Research Center, 63 Nguyen Van Huyen, Ha Noi 100000, Vietnam, binhnhiduong@gmail.com (T.X.D.)
[4] Optical Science and Engineering, Fudan University, Shanghai 200433, China, lychen@fudan.ac.cn (L.C.)
[5] Department of Physics, Quantum Photonic Science Research Center and RINS, Hanyang University, Seoul 04763, Republic of Korea, haiyu@hanyang.ac.kr (H.Z.)
[6] Alpha ADT Co., Ltd., Hwaseong 18469, Republic of Korea
* Correspondence: yplee@hanyang.ac.kr (Y.P.L.)
** Co-correspondence: tungdk@ims.vast.ac.vn (D.K.T.); tungbs@ims.vast.ac.vn (B.S.T)

Abstract: This study presents a tri-layer broadband metamaterial absorber which operates in the GHz range. The absorber was composed of a polyhedral iron-cobalt alloy/graphite nanosheet material arranged in a flat sheet with two punched-in rings for the top layer, a continuous FR-4 layer at the middle, and a continuous copper layer at the bottom. For the normal incidence of electromagnetic wave, the proposed absorber demonstrated an exceptional broadband absorption in a frequency range of 7.9-14.6 GHz, revealing an absorption exceeding 90%. The absorption magnitude remains to be above 90% in a frequency range of 8-11.1 GHz for transverse-electric-polarized waves at incident angles up to 55°. For both transverse-magnetic- and electric-polarized waves, the absorption exceeds 90% in a frequency range of 9.5-14.6 GHz. The physical mechanism behind the absorption properties is analyzed thoroughly through the electric- and magnetic-field distributions. The obtained results could contribute potentially to the development of microwave applications based on metamaterial absorbers, such as radar-stealth technology, electromagnetic shielding for health safety and reduced electromagnetic interferences for high-performance communications and electronic devices.

Keywords: metamaterials; broad-band absorption; iron-cobalt alloy; electromagnetic coupling

1. Introduction

The microwave metamaterial absorbers (MAs) became to be an emerging class of materials which have shown great potential in applications such as electromagnetic (EM)-wave absorption, stealth technology, and energy harvesting [1]. These artificial materials consisted of sub-wavelength unit cells which was designed to interact with incident EM waves, leading to an efficient absorption [2,3]. The absorption mechanism depends on the specific design and constituent materials of metamaterial structure [4]. A significant challenge in the microwave MA is the extension of absorption bandwidth, particularly, towards higher frequencies. Researchers have developed several strategies to overcome this challenge [5–7]. One approach includes the design of MA structures with multiple resonant modes, which might expand the absorption spectrum. Another way is to use multilayer structures with varying materials and thicknesses, leading to a gradient of the effective permittivity and permeability, which results in a broad absorption bandwidth.

 doi:10.20944/preprints202306.0371.v1

The recent research has focused on the employment of FeCo and nano-carbon materials for the microwave absorption applications. The FeCo-based materials have shown high magnetic permeability and can be magnetized easily, making them well-suited for the microwave absorbers based on the magnetic loss [8–10]. Conversely, the nano-carbon materials, such as carbon nanotubes or graphene, have a high electrical conductivity and can be used for the absorbers in terms of resistive loss [11–15]. Therefore, the incorporation of FeCo nanoparticles into the carbon-based materials, has been shown to improve the magnetic loss significantly, while the kind of materials can enhance the electrical conductivity [16–19]. Overall, the use of alloys might lead to the development of more efficient and effective microwave absorbers.

In our work, by exploiting both usual MA and alloy, a novel FeCo/carbon-based metamaterial structure is presented to enhance the microwave absorption. The simulated results demonstrate a remarkable improvement in the absorption bandwidth of proposed MA, compared with that of FeCoC plate backed by the bare copper. We clarify the absorption mechanism by investigating the electric- and magnetic-field distribution and study the contribution of losses in the MA. Moreover, the effects of polarization and incident angle on the absorption are examined to evaluate the operational performance of proposed MA.

2. Structural Design and Methods

Figure 1 shows the schematic of proposed MA, featuring the optimized design for the unit cell. The structure comprises three layers: FeCo/graphite nanosheets (FeCo-C) whose shape looks like a flat sheet with two punched-in rings at the top, a middle layer of FR-4, and a continuous copper plate at the bottom. In our simulation, we used a relative permittivity of FR-4 of 4.3, with a loss tangent of 0.025, and employed the copper layer with a conductivity of 5.8×10^7 S/m. We utilized the polyhedral FeCo/graphite nanosheet material, whose frequency-dependent complex permittivity and permeability were determined experimentally by Xiaogang Su et al. [20], as indicated in Figure 2.

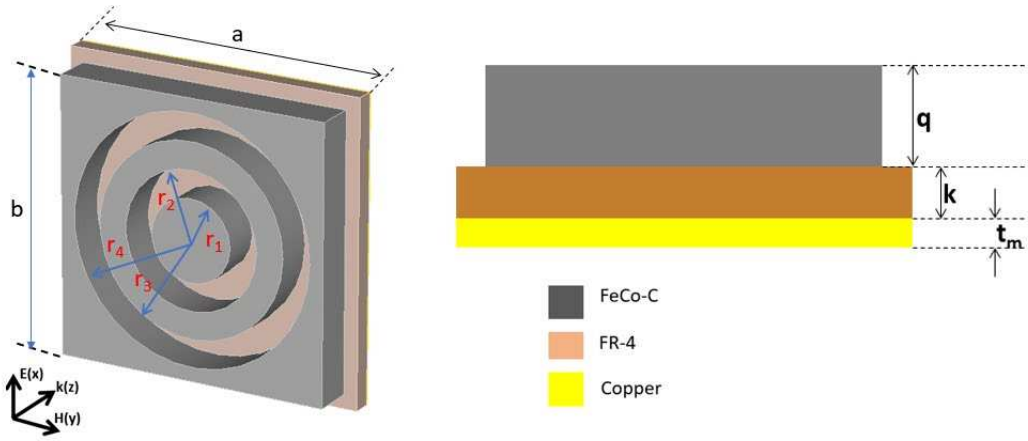

Figure 1. Schematic of the proposed unit cell with the optimized geometrical parameters. a = 22, b = 20, r_1 = 3, r_2 = 5, r_3 = 7, r_4 = 9, q = 3, k = 0.5, t_m = 0.036 mm.

We used the CST Microwave Studio software [21] to conduct the simulation, employing the frequency domain solver in a frequency range from 1 to 15 GHz. To impose the periodic boundary conditions, we utilized the x- and y-direction. The absorption was calculated by using formula $A(\omega) = 1 - R(\omega) - T(\omega)$, where $R(\omega) = |S_{11}(\omega)|^2$ and $T(\omega) = |S_{21}(\omega)|^2$ were the reflection and transmission, respectively. In our design, the bottom layer was composed of a continuous copper plate, resulting in zero transmission in the microwave region, and thus the absorption becomes simply to be $A(\omega) = 1 - R(\omega)$.

Preprints.org (www.preprints.org) | NOT PEER-REVIEWED | Posted: 6 June 2023 doi:10.20944/preprints202306.0371.v1

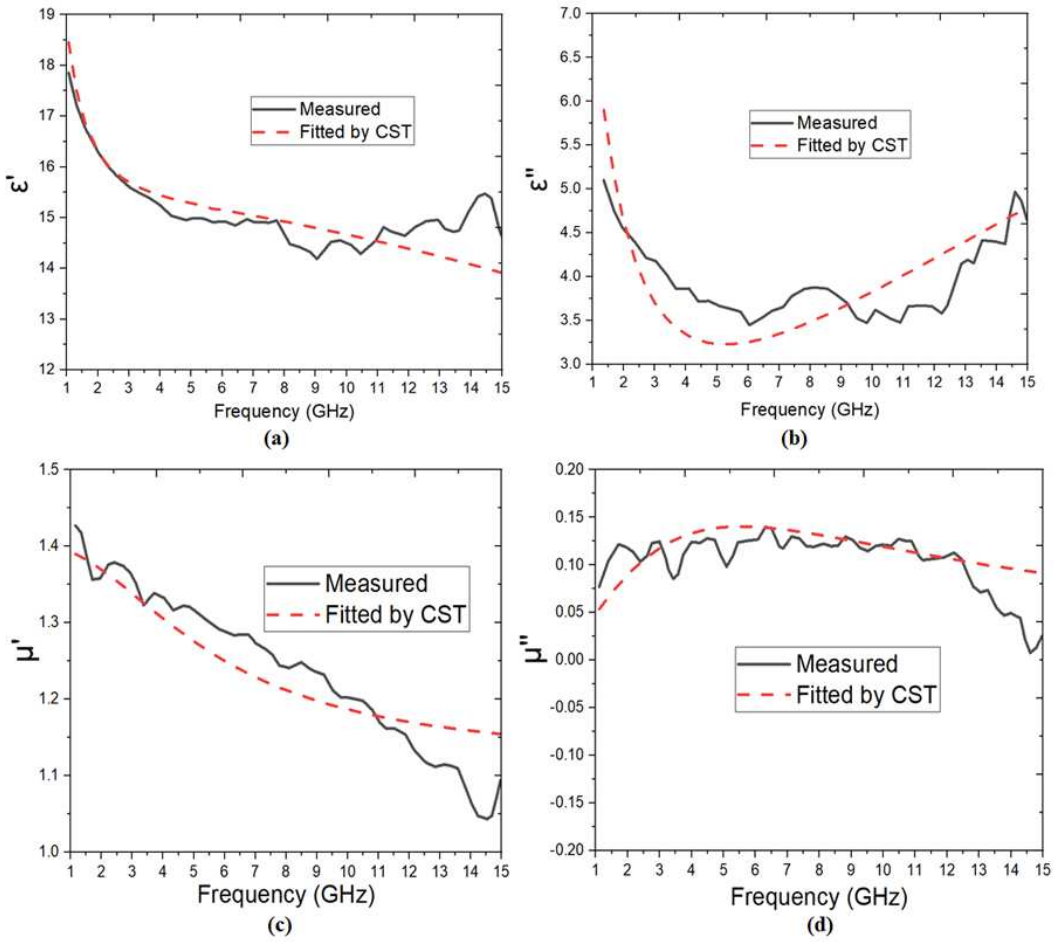

Figure 2. Frequency-dependence of the complex permittivity and permeability of FeCo-C. (**a**) Real ε′ and (**b**) imaginary ε″ parts of the permittivity. (**c**) Real μ′ and (**d**) imaginary μ″ parts of the permeability. The corresponding measured data are employed from Ref. 20 for the fitting.

3. Results and Discussion

As the initial step, we examined the reflection-loss properties of FeCo-C material, which was utilized on a copper plate [Figure 3(a)]. The thickness of FeCo-C layer was changed gradually from 1.6 to 5.3 mm in Figs. 3(b) and 3(c). That of the copper plate was t_m = 0.036 mm. Figures 3(b) and 3(c) display the simulated reflection loss and absorption spectrum, respectively, of FeCo-C according to the layer thickness, which was backed by the copper plate. Our simulated results are in accordance with the reported results in Ref. 20.

Figure 4(a) shows the absorption spectrum of MA, based on FeCo-C. The proposed structure exhibits a broadband absorption, with an absorption over 90% in a frequency range of 7.9 to 14.6 GHz, featuring two peaks with the near-unity absorption at 9.4 and 12.5 GHz, respectively. The absorption spectrum of the FeCo-C-based MA was found to be significantly broader than that of the copper-backed FeCo-C, indicating an improvement in the absorption upon integrating the FeCo-C material into the metamaterial structure. To clarify the role of different layers in the metamaterial structure, the fractions of energy dissipated in the FeCo-C and FR-4 layer are presented in Figure 4(b). It is shown that more than 98% of the energy loss occurred in the FeCo-C layer, while the loss in the FR-4 one was limited to be only 2%. The energy-dissipation results prove that the FeCo-C layer in MA is the main factor contributing to the broadband absorption.

Preprints.org (www.preprints.org) | NOT PEER-REVIEWED | Posted: 6 June 2023 doi:10.20944/preprints202306.0371.v1

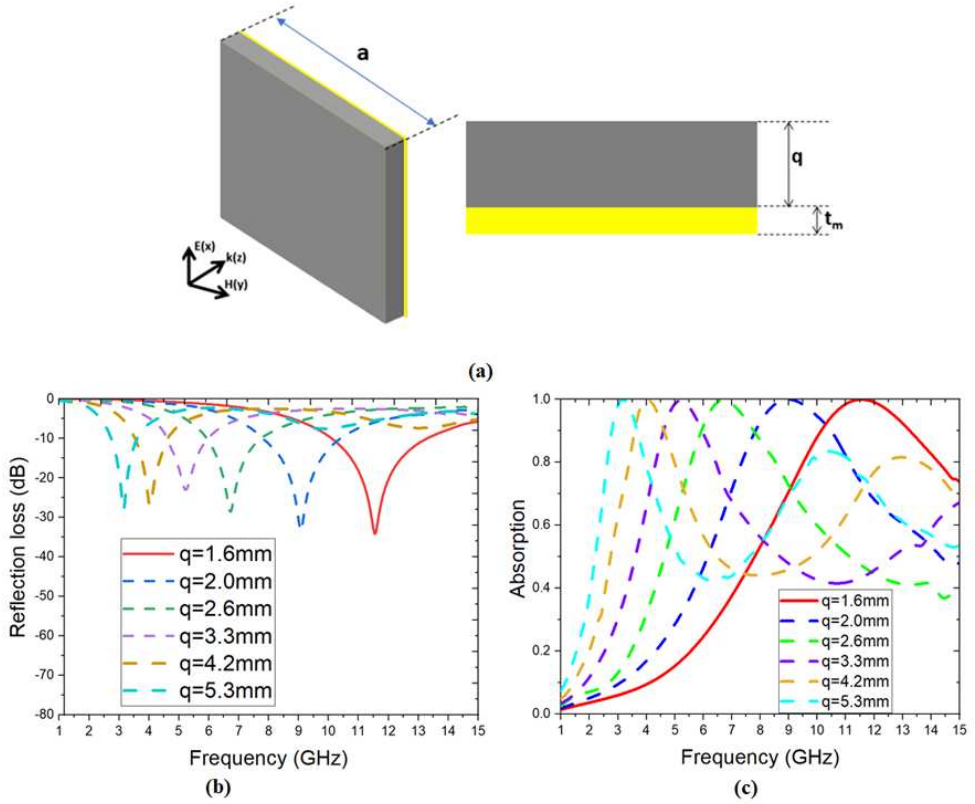

Figure 3. (**a**) Schematic of the FeCo-C structure backed by the copper plate. (**b**) Reflection-loss curve and (**c**) the corresponding absorption spectrum for different layer thicknesses.

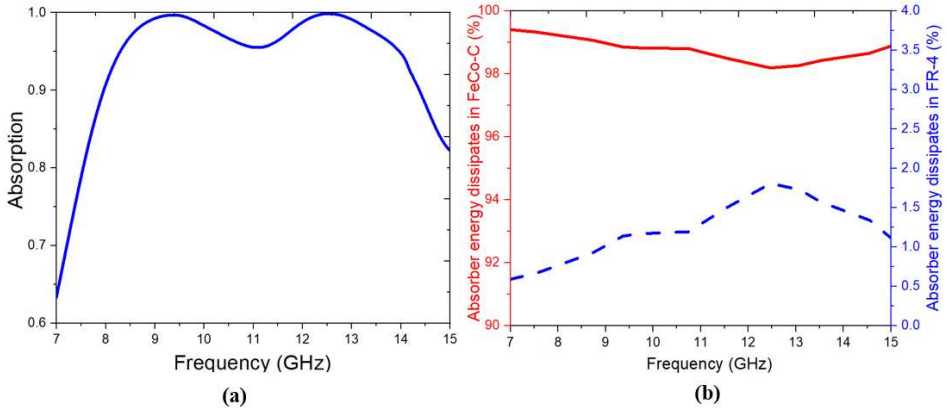

Figure 4. (a) Absorption spectrum of the designed MA structure and (b) the captured energy dissipated in the FeCo-C and FR-4 layer in the MA structure.

As shown in Figure 4, the strongest absorption peaks are located at 9.4 and 12.5 GHz. Therefore, the distributions of electric and magnetic field at these frequencies are presented in Figs. 5 and 6 to clarify the nature of absorption. Figures 5(a) and 5(b) show that of the magnetic field in the (**E**, **H**) and (**H**, **k**) planes, respectively, at the lower absorption frequency of 9.4 GHz. The corresponding one of electric field in the (**E**, **k**) plane is in Figure 5(c). It can be observed that the magnetic field is strongly excited at the corners of MA structure. Specifically, the magnetic dipoles are seen along the direction of incident **H**-field with electric half vortices at the same positions. The observed phenomena suggest that the absorption mode at 9.4 GHz is due to a magnetic-dipole Mie-resonance, caused by the dielectric resonator [22–27]. Figure 6 presents the distributions of electric and magnetic field in different planes at 12.5 GHz. The MA also exhibits the magnetic-dipole Mie-resonance, as indicated

 doi:10.20944/preprints202306.0371.v1

by the strong magnetic dipoles along the **H**-direction and the electric half vortices in the (**E**, **k**) plane. However, the locations of magnetic dipoles at 12.5 GHz differ from those at 9.4 GHz. As shown in Figure 6, the induced magnetic dipoles are distributed in both center and outer edges of the MA structure, which are, of course, parallel to the **H**-direction.

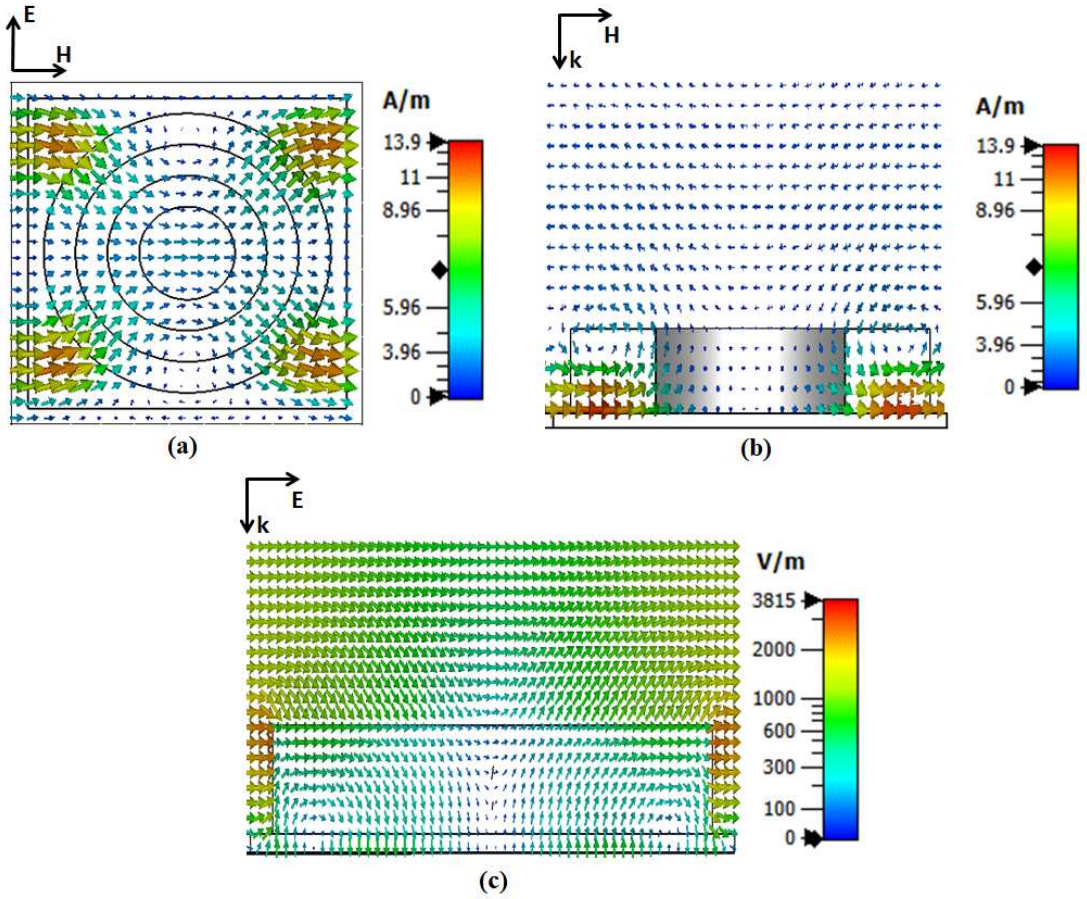

Figure 5. Electric- and magnetic-field distribution of the MA structure. (**a**) Magnetic field in the (**E**, **H**) plane, (**b**) magnetic field in the (**H**, **k**) plane and (**c**) electric field in the (**E**, **k**) plane at a frequency of 9.4 GHz.

Preprints.org (www.preprints.org) | NOT PEER-REVIEWED | Posted: 6 June 2023 doi:10.20944/preprints202306.0371.v1

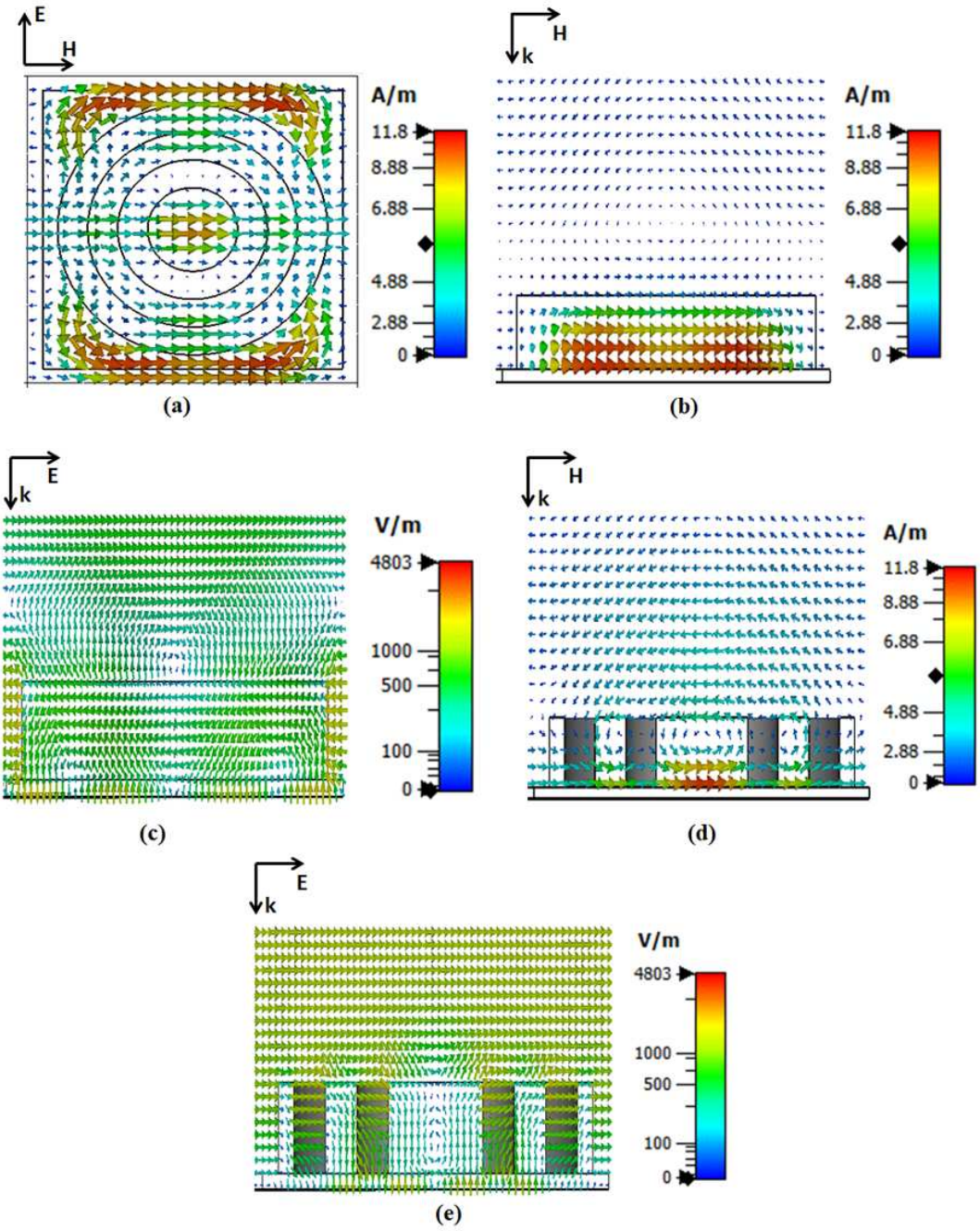

Figure 6. Electric- and magnetic-field distributions of the MA structure at a frequency of 12.5 GHz. (**a**) Magnetic field in the (**E**, **H**) plane. (**b**) and (**d**) Magnetic field in the (**H**, **k**) plane. (**c**) and (**e**) Electric field in the (**E**, **k**) plane.

To investigate the role of the real and imaginary parts of the complex permittivity (ε′ and ε″) in the absorption mechanism, we analyzed the absorption characteristics of MA structure by reducing the ε′ and ε″ value to be 1/2, 1/4 and 1/6 of the original value, as illustrated in Figure 7. Initially, for the original ε′ and ε″ values in Figure 2, the absorption spectrum showed a wide bandwidth of 7.9-14.6 GHz with an absorption exceeding 90%. As the ε′ value is decreased, the absorption of structure also decreases and the absorption peak shifts to a higher-frequency region [Figure 7(a)]. In addition, the reduction of ε″ value results in the change of absorption spectrum to be from the wideband to multi-band absorption [Figure 7(b)]. These results suggest that the real part of FeCo-C permittivity defines mainly the frequency range of absorption spectrum, while the imaginary part is responsible for the bandwidth of absorption.

Preprints.org (www.preprints.org) | NOT PEER-REVIEWED | Posted: 6 June 2023 doi:10.20944/preprints202306.0371.v1

We also investigated the role of the real and imaginary parts of the complex permeability (μ′ and μ′′) on the absorption mechanism. The absorption characteristics of MA structure according to the values of μ′ and μ′′ were simulated, as shown in Figure 8. Similarly, to the reduction of the real part of permittivity, lowering the μ′ value causes a shift of the absorption spectrum towards a higher-frequency range. However, the results in Figure 7(b) indicate that reducing the imaginary-part μ′′ value does not change significantly the absorption spectrum of MA.

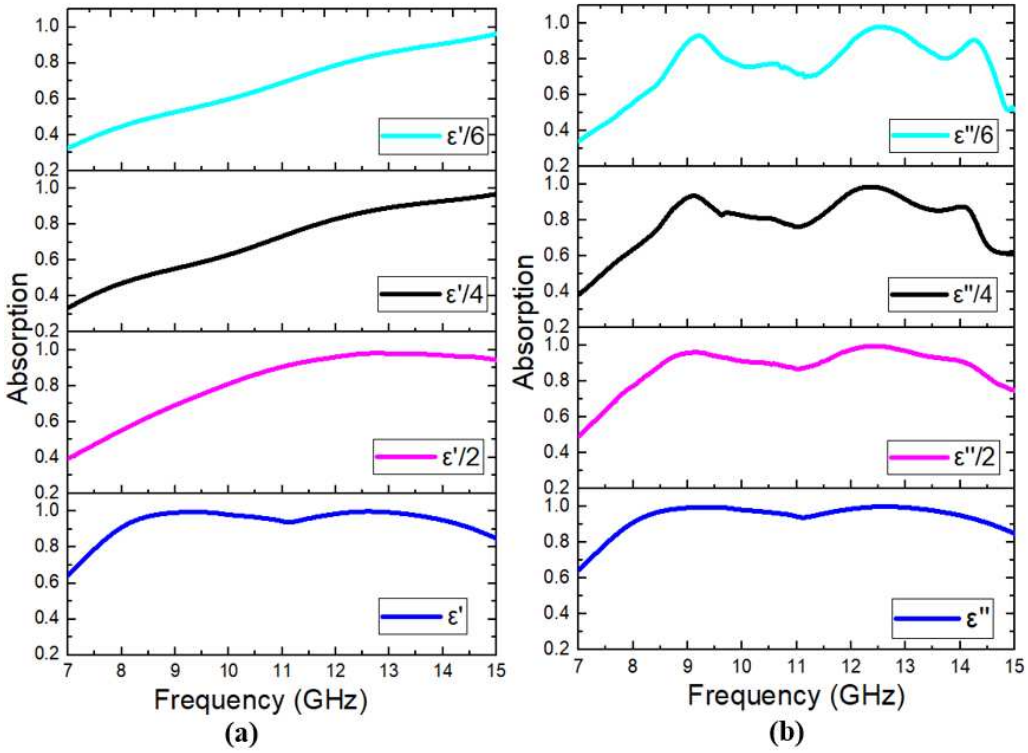

Figure 7. Absorption spectra of the MA corresponding to the (**a**) real and (**b**) imaginary parts of FeCo-C permittivity.

To evaluate the performance of proposed MA structure, we also investigated the absorption spectra by varying incident angle and polarization of incoming EM wave. We found that the absorption spectrum was largely unaffected by the change in polarization angle owing to the inherent symmetry of structure, as shown in Figure 9(a). However, the absorption of MA is influenced by the incident angle, as indicated by a reduction in both absorption magnitude and bandwidth [see Figs. 9(b) and 9(c)]. Nonetheless, the proposed MA still reveals a good absorption property for both transverse-electric (TE) and transverse-magnetic (TM) polarization even at large incident angles. Specifically, for the TE polarization, the absorption decreases as the incidence angle increases from 0 to 55° but remains higher than 90% in a frequency range of 8 to 11.1 GHz, as shown in Figure 9(b). Similarly, in the TM mode, the absorption is maintained to be higher than 90% in a frequency region of 9.5 to 14.6 GHz for incident angles up to 55°, as demonstrated in Figure 9(c). These results reveal the high performance of proposed MA, which is insensitive to the polarization of incoming EM wave and highly stable under the oblique incidence.

Preprints.org (www.preprints.org) | NOT PEER-REVIEWED | Posted: 6 June 2023 doi:10.20944/preprints202306.0371.v1

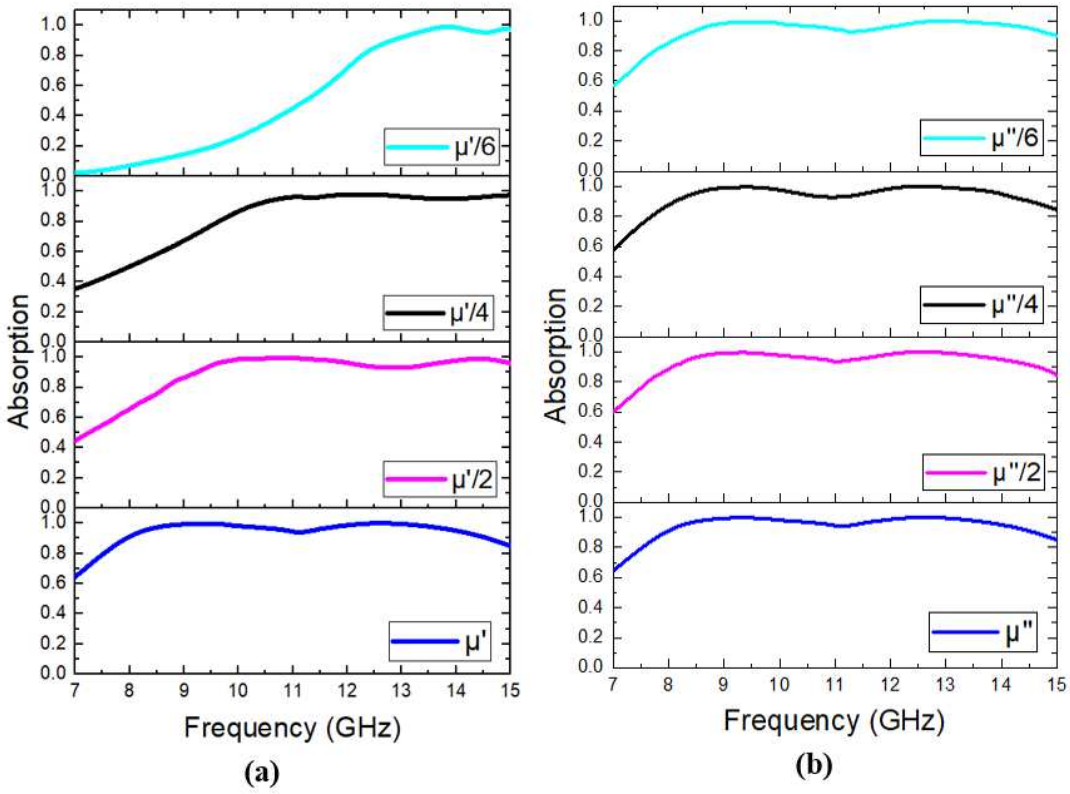

Figure 8. Absorption spectra of MA corresponding to the (**a**) real and (**b**) imaginary parts of FeCo-C permeability.

Finally, the absorption properties of proposed MA are compared with those of other absorbers reported previously (shown in Table 1), such as plain FeCo-C composites [20], FeCo/ZnO ones [28], Fe_3C/C nanofibers [29], and snowflake-like MnO_2@$NiCo_2O_4$ ones [30]. The efficient bandwidth (EBW) of absorption is calculated as follows.

$$EBW = f_{high} - f_{low} \quad (1)$$

where f_{high} and f_{low} are the highest and lowest frequencies where the absorption is greater than 90%, respectively. The results indicate that our proposed absorber exhibits an enhanced absorption bandwidth, which can be attributed to not only the intrinsic properties of FeCo-C material but also the exploitation of MA structure.

Table 1. Comparison of the microwave absorption bandwidth of proposed MA with those of other absorbers of different materials in previous studies.

Samples	EBW of absorption (GHz)	Reference
FeCo/ZnO	5.1	[28]
Fe_3C/C	4.5	[29]
MWCNTs/$NiFe_2O_4$	3.8	[30]
plain FeCo-C	4.3	[20]
MA-based FeCo-C	6.7	This work

 doi:10.20944/preprints202306.0371.v1

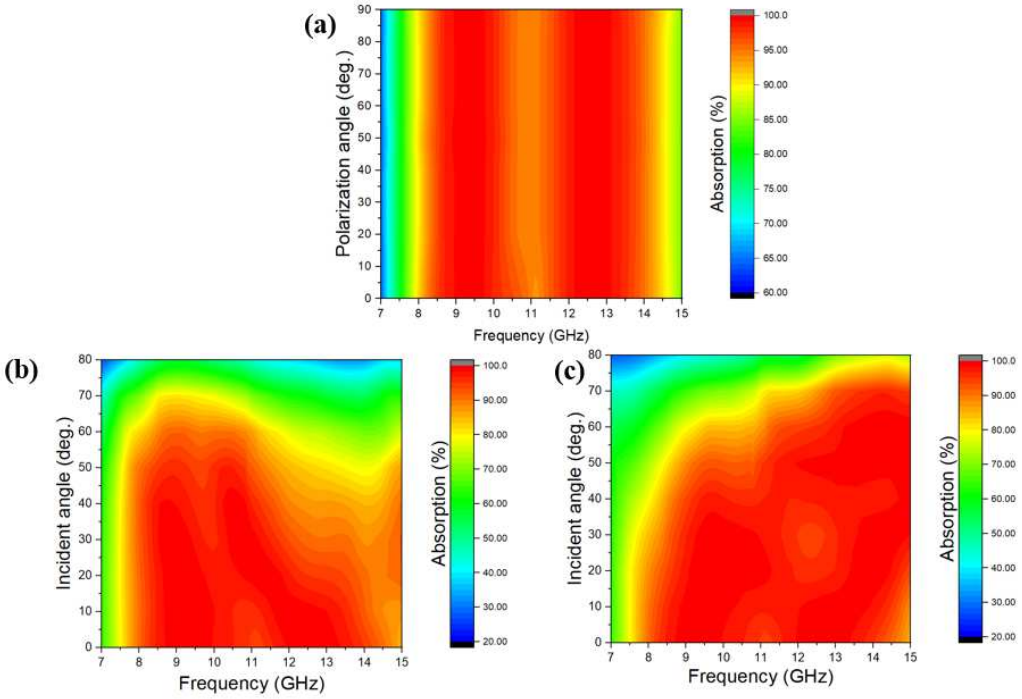

Figure 9. Dependence of the absorption spectrum of proposed MA on the (**a**) polarization angle at the normal incidence, and incident angle in the (**b**) TE and (**c**) TM polarization.

4. Conclusions

We demonstrated that the EM-wave absorption properties of FeCo-C alloy were enhanced by exploiting the metamaterial structure. The ultrabroadband absorption was achieved between 7.9 and 14.6 GHz, with an absorption above 90% in case of the normal incidence of incoming EM wave for all polarization angles. The absorption remains to be above 90% in a frequency range of 8-11.1 GHz at wide angles of incidence from 0 to 55° for the TE polarization, while in the TM mode the absorption was also over 90% in a frequency range of 9.5-14.6 GHz. The physical mechanism of proposed MA was elucidated, revealing that the high and ultrabroadband absorption was controlled by the magnetic-dipole Mie-resonances in the MA structure and the intrinsic EM properties of FeCo-C material. Our work might contribute to the exploitation of various materials for the development of future MAs, which are used potentially for the microwave applications in radar and telecommunication technology, as well as for EM shielding for health safety.

Author Contributions: T.X.D., B.S.T., B.X.K., V.D.L. and Y.P.L. conceived the idea. The electromagnetic simulation and calculation were carried out by T.X.D, B.S.T., B.X.K., N.T.N.A. and H.Z. D.K.T., B.S.T., B.X.K., L.C., Y.P.L. and V.D.L. analyzed and wrote the article. All of the authors discussed and commented on the manuscript. All authors have read and agreed to the published version of the manuscript.

Funding: This research is funded by Vietnam Academy of Science and Technology, under grant number VAST03.01/22-23, and by the Korea Evaluation Institute of Industrial Technology (Project No. 20016179).

Institutional Review Board Statement: Not applicable.

Informed Consent Statement: Not applicable.

Data Availability Statement: The data presented in this paper are available on request from the corresponding author.

Conflicts of Interest: The authors declare no conflict of interest. The funders had no role in the design of the study; in the collection, analyses, or interpretation of data; in the writing of the manuscript, or in the decision to publish the results.

References

1. Abdulkarim, Y.I.; Mohanty, A.; Acharya, O.P.; Bhargav, A.; Khan, M.S.; Mohapatra, S.K.; Muhammadsharif, F.F; Dong, J. A Review on Metamaterial Absorbers: Microwave to Optical. *Front. in Phys.* 2022, 10, 893791.
2. Bregar, V.B.; Znidarsic, A.; Lisjak, D.; Drofenik, M. Development and Characterisation of an Electromagnetic Absorber. *Mat. in Teh.* 2005, 39, 89–93.
3. Li, S.; Qiao, X.; Chen, J. Nano-Composite Electromagnetic Wave Absorbers. *J. Astr.* 2006, 27, 317-322.
4. Li, Y.; Liu, X. F.; Nie, X. Y.; Yang, W. W.; Wang, Y. D.; Yu, R. H. Multifunctional Organic–Inorganic Hybrid Aerogel for Self-Cleaning, Heat-Insulating, and Highly Efficient Microwave Absorbing Material. *Adv. Funct. Mater.* 2018, 29, 1807624.
5. Landy, N. I.; Sajuyigbe, S.; Mock, J. J.; Smith, D. R.; Padilla W. J. Perfect Metamaterial Absorber. *Phys. Rev. Lett.* 2008, 100, 207402.
6. Hai, L. D; Qui, V.D; Tung, N.H.; Huynh, T.V; Dung, N.D; Binh, N.T; Tuyen, L.D.; Lam, V.D. Conductive polymer for ultra-broadband, wide-angle, and polarization-insensitive metamaterial perfect absorber. *Opt. Expr.* 2018, 26(25), 33253.
7. Akselrod, G.M.; Huang, J.; Thang B.H.; Bowen; P.T.; Su, L.; Smith, D.R.; Mikkelsen, M.H. Large-Area Metasurface Perfect Absorbers from Visible to Near-Infrared. *Adv. Mater.* 2015, 27, 8028–8034.
8. Park, J.H.; Park, C.; Lee, K.S.; Suh, S.J. Effect of NaOH and precursor concentration on size and magnetic properties of FeCo nanoparticles synthesized using the polyol method. *AIP Adv.* 2020, 10 (11), 115220.
9. Liu, X.G.; Geng, D.Y.; Meng, H.; Li, B.; Zhang, Q.; Kang, D.J.; Zhang, Z.D. Electromagnetic-wave-absorption properties of wire-like structures self-assembled by FeCo nanocapsules. *J. Phys. D. Appl. Phys*. 2008, 41, 175001.
10. Cheng, Y.; Ji, G.; Li, Z.; Lv, H; Liu, W.; Zhao, Y.; Cao, J.; Du, Y. Facile synthesis of FeCo alloys with excellent microwave absorption in the whole Ku-band: Effect of Fe/Co atomic ratio. *J. Alloys Compd.* 2017, 704, 289–295.
11. Wen, B.; Cao, M. S.; Hou, Z. L.; Song, W. L.; Zhang, L.; Lu, M. M. Temperature Dependent Microwave Attenuation Behavior for Carbon-Nanotube/Silica Composites. *Carbon.* 2013, 65, 124–139.
12. Kim, S. H.; Park, Y. G.; Kim, S. S. Double-Layered Microwave Absorbers Composed of Ferrite and Carbon Fiber Composite Laminates. *Phys. Stat. Sol. C.* 2007, 4, 4602–4605.
13. Chen, H.; Ma, W.; Huang, Z.; Zhang, Y.; Huang Y.; Chen, Y. Graphene-Based Materials toward Microwave and Terahertz Absorbing Stealth Technologies. *Adv. Opt. Mat.* 2019, 7, 1801318.
14. Huang, Z.; Chen, H.; Huang, Y.; Ge, Z.; Zhou, Y.; Yang, Y.; Xiao, P.; Liang, J.; Zhang, T.; Qian, S.; Li, G.; Chen, Y. Ultra-Broadband Wide-Angle Terahertz absorption properties of 3D graphene foam. *Adv. Funct. Mat.* 2018, 28, 1704363.
15. Zhang, Y.; Huang, Y.; Chen, H. H.; Huang, Z. Y.; Yang, Y.; Xiao, P. S.; Zhou, Y.; Chen, Y. S. Composition and Structure Control of Ultralight Graphene Foam for High-Performance Microwave Absorption. *Carbon*. 2016, 105, 438–447.
16. Han, Z.; Li, D.; Wang, H.; Liu, X.G.; Li, J.; Geng, D.Y.; Zhang, Z.D. Broadband electromagnetic-wave absorption by FeCo/C nanocapsules, *Appl. Phys. Lett.* 2009, 95, 16–19.
17. Han, Z.; Li, D.; Wang, X.W.; Zhang, Z.D. Microwave response of FeCo/carbon nanotubes composites. *J. Appl. Phys.* 2011, 109, 2009–2012.
18. Jiang, J.J.; Li, X.J.; Han, Z.; Li, D.; Wang, Z.H.; Geng, D.Y.; Ma, S.; Liu, W.; Zhang, Z.D. Disorder-modulated microwave absorption properties of carbon-coated FeCo nanocapsules. *J. Appl. Phys.* 2014, 115, 2012–2015.
19. Lv, H.; Ji, G.; Zhang, H.; Li, M.; Zuo, Z.; Zhao, Y.; Zhang, B.; Tang, D.; Du, Y. Co_xFe_y@C Composites with Tunable Atomic Ratios for Excellent Electromagnetic Absorption Properties. *Sci. Rep.* 2015, 5, 1–10.
20. Su, X.G.; Wang, J.; Zhang, X.X.; Huo, S.Q.; Dai, W.; Zhang, B. Synergistic effect of polyhedral iron-cobalt alloys and graphite nanosheets with excellent microwave absorption performance. *J. Alloys Compd.* 2020, 829, 154426.
21. CST Microwave Studio 2019, License ID: 52856-1. Dassault Systemes. Available online: http://www.cst.com (accessed on 15 June 2021).
22. Bohren, C. F.; Huffman, D. R. *Absorption and scattering of light by small particles*, John Wiley & Sons, New York, 2008.

 doi:10.20944/preprints202306.0371.v1

23. Wang, Q.; Zhang, F.; Xiong, Y.J.; Wang, Y.; Tang, X.Z; Jiang, C. Abrahams, I.; Huang X Z. Dual-band binary metamaterial absorber based on low-permittivity all-dielectric resonance surface. *J. Electron. Mat.*2019, 48, 787-793.
24. Zhang, F.; Jiang, C.; Wang, Q.; Zhao, Z.; Wang, Y.; Du. Z.; Wang, C.; Huang, X. A multi-band closed-cell metamaterial absorber based on a low-permittivity all-dielectric structure *Appl. Phys. Express*, 2020,13, 084001.
25. Guo, M.Ch.; Wang, X.K.; Zhuang, H.Y.; Tang, D.M.; Zhang, B.S.; Yang, Y. 3D printed low-permittivity all-dielectric metamaterial for dual-band microwave absorption based on surface lattice resonances. *Phys. Scrip.* 2022, 97, 075504.
26. Zhu, Y.Q.; Tian, X.; Fang, J.K.; Shi, Y.P.; Shi, S.N.; Zhang, S.; Song, J.M.; Li, M.P.; Liu, X.Y.; Wang, X.D.; Yang, F.H. Independently tunable all-dielectric synthetic multi-spectral metamaterials based on Mie resonance. *RSC Adv*. 2022, 12, 20765-20770.
27. Zhao, Q.; Kang, L.; Du, B.; Zhao, H.; Xie, Q.; Huang, X.; Li, B.; Zhou, J.; Li, L. Experimental Demonstration of Isotropic Negative Permeability in a Three-Dimensional Dielectric Composite. *Phys. Rev. Lett.* 2008, 101, 027402.
28. Bao, X.; Wang, X.; Zhou, X.; Shi, G.; Xu, G.; Yu, J.; Guan, Y.; Zhang, Y.; Li, D.; Choi, C. Excellent microwave absorption of FeCo/ZnO composites with defects in ZnO for regulating the impedance matching. *J. Alloys Compd.* 2018, 769, 512-520.
29. Jiang, Y.; Fu, X.; Zhang, Z.; Du, W.; Xie, P.; Cheng, C.; Fan, R. Enhanced microwave absorption properties of Fe_3C/C nanofibers prepared by electrospinning. *J. Alloys Compd.* 2019, 804, 305-313.
30. Wei, S.; Wang, X.; Zheng, Y.; Chen, T.; Zhou, C.; Chen, S.; Liu, J. acile preparation of snowflake-like MnO_2@$NiCo_2O_4$ composites for highly efficient electromagnetic wave absorption. *Chem. Eur. J.* 2019, 25, 7695-7701.